frontiers in Materials

METHODS
published: 06 October 2020
doi: 10.3389/fmats.2020.00277

Study on Flexural Properties of Basalt Fiber Textile Reinforced Concrete (BTRC) Sheets Including Short AR-Glass Fibers

Qin Zhang[1,2,3], Sanya Li[1], Susu Gong[1], Guanhua Zhang[2], Guangheng Xi[2] and Yaoqing Wu[1]*

[1] College of Civil and Transportation Engineering, Hohai University, Nanjing, China, [2] Liaoning Provincial Traffic Planning and Design Institute Co., Ltd., Shenyang, China, [3] College of Civil Engineering, Tongji University, Shanghai, China

OPEN ACCESS

Edited by:
Prabir Kumar Sarker, Curtin University, Australia

Reviewed by:
Ping Duan, China University of Geosciences Wuhan, China
Yue Zhang, Qingdao University of Technology, China

***Correspondence:**
Qin Zhang
qinzhang8190@gmail.com; zhangqin8190@163.com

Specialty section:
This article was submitted to Structural Materials, a section of the journal Frontiers in Materials

Received: *15 April 2020*
Accepted: *24 July 2020*
Published: *06 October 2020*

Citation:
Zhang Q, Li S, Gong S, Zhang G, Xi G and Wu Y (2020) Study on Flexural Properties of Basalt Fiber Textile Reinforced Concrete (BTRC) Sheets Including Short AR-Glass Fibers. Front. Mater. 7:277. doi: 10.3389/fmats.2020.00277

Experimental investigations were carried out to determine the mechanical properties of fine-grained concrete with short AR-glass fibers including the effects of fiber content and length. The basalt fiber textile reinforced concrete (BTRC) sheets with short AR-glass fibers were tested under four-point bending, and the effects of the number of textile layers and fiber length on the flexural properties were analyzed. The results show that the mechanical properties of fine-grained concrete with fibers were mainly related to fiber length and content, the mechanical properties of fibers reinforced concrete increase with the increase of fiber length, and the comprehensive mechanical properties of fine-grained concrete materials are the best when the AR-glass fiber content is about 5%. The flexural performance tests of BTRC sheets show that the strength and the deformation capacity of sheets increase with the increase of the number of fiber textile layers. The short AR-glass fibers can also effectively improve the strength and deformation capacity of BTRC sheets, and the cracking load and ultimate displacement can be increased by up to 1.1 times and 10.1 times of the sheet without short fibers, respectively. For the multi-fiber compound reinforced concrete sheets, the fiber textile can provide tension in the desired direction, and the short AR-glass fibers can improve the cracking resistance and toughness of sheets.

Keywords: basalt fiber textile reinforced concrete, sheets, short AR-glass fibers, flexural properties, mechanical performance

INTRODUCTION

Textile-reinforced concrete (TRC) is a cement-based composite material with high-performance two-directional or multi-directional continuous fiber textiles as reinforcement and with inorganic cementitious material as a matrix, which exhibits features including good tensile properties, directional mechanical performance, and easy casting molding (Hegger et al., 2006; Yin et al., 2014). Moreover, TRC composites are compatible with concrete substrate and more suitable for wet and

low-temperature environments than fiber-reinforced polymer (FRP) systems since the inorganic cementitious material is adopted as the bonding agent (Al-Salloum et al., 2011; Wang et al., 2020). Currently, TRC has grown in popularity when applied in the thin-walled form both for new construction and for repairing existing structures (Di Ludovico et al., 2012; Isabella et al., 2013; Pellegrino and D'Antino, 2013). The primary forms of TRC include CTRC (i.e., carbon textile reinforced concrete), GTRC (i.e., glass textile reinforced concrete) and BTRC (i.e., basalt textile reinforced concrete) according to the different types of textile used for reinforcement in the composites (Zhu et al., 2011, 2009; Dvorkin et al., 2013). For CTRC and GTRC, many studies have been carried out in the past decade, concentrating on the mechanical properties and their application in strengthening and restoration. However, few studies have focused on the mechanical performance and application of BTRC materials. In fact, basalt fiber is an inorganic fiber with high strength, high temperature resistance, excellent stability, good chemical resistance, and is non-toxic, natural, eco-friendly, inexpensive, and easy to process (Dhand et al., 2015). Furthermore, the economic efficiency is much better compared to the use of carbon counterparts, and the properties are more tensile and utility-friendly than AR-glass fibers (Szabó and Czigány, 2003; Liu et al., 2006; Carmisciano et al., 2011). Thus, it is preferable to use basalt fiber textile to strengthen fine-grained concrete to form composite materials compared with textile composed of carbon and glass fiber. Recently, Larrinaga et al. (2014); Rambo et al. (2015), and Du et al. (2017) separately studied the mechanical properties of BTRC composites subjected to tensile loading. The results indicated that BTRC composites have superior tensile properties, and their ultimate strains are far beyond 3%, and the behavior of BTRC is strongly affected by the number of textile layers. However, studies on the bending properties, ductility as well as toughness of BTRC are relatively limited. Therefore, it is very necessary to study the bending behavior of BTRC and its affecting factors.

To improve the disadvantages including easy cracking and poor toughness of the traditional TRC matrix in application, many scholars have tried to develop high-toughness TRC composites by adding short fibers into the matrix. Halvaei et al. (2020) studied the effects of volume content and short carbon fiber length on flexural properties of high-toughness CTRC. The four-point bending test indicated that cracking loads and ultimate loads, as well as the flexural toughness of CTRC significantly increased with an increase in the volume content of fiber. Li and Xu (2011) investigated the mechanical performance of carbon-textile-reinforced cementitious composites with short PVA fiber, and the bending tests were carried out. The results showed that the integrated performance of CTRC, particularly cracking response, is evidently influenced by the volume content of PVA fiber, and composites with 1.5% PVA fiber behave much better than those with 1.0% PVA fiber. Shen et al. (2016) and Yin et al. (2016, 2019) separately studied the impact of the types of short fibers on flexural behavior of CTRC and found that the cross-linking effect of short fibers could improve the bonding performance of the interface between the textile and matrix. Moreover, Barhum and Mechtcherine (2012, 2013a) studied the strength, deformation, and fracture behavior of thin sheets made of GTRC both with and without the addition of short fibers by a series of uniaxial, deformation-controlled tension tests. The results showed that the first-crack stress is increased due to the addition of short dispersed fibers, and the tensile strength of GTRC samples is improved with the addition of short fibers. Zhu et al. (2019) and Li et al. (2020) separately investigated the tensile behaviors of BTRC with different layers of textile, and the effect of short fibers and pre-tension were also considered in their studies. Results indicated that first crack stress and toughness are significantly improved by short fibers and pre-tension. Deng et al. (2020) studied the impact of the textile reinforcing ratio and the volume content of short PVA fibers on the tensile mechanical behavior of CTRC, and the experimental results indicated that the PVA fibers could significantly improve the bond properties between carbon textile and matrix, as well as increase the tensile strength and strain. Furthermore, the hybridization of glass textiles with carbon fiber and its effects on the tensile properties of the composites have also been investigated (Hinzen and Brameshuber, 2009; Barhum and Mechtcherine, 2013b). These studies indicated that the cracking resistance and toughness of the matrix are improved through the application of short fibers. Although the comprehensive behavior of TRC is further enhanced by combination with short fibers, studies about the effect of short fibers on the mechanical behavior of BTRC are relatively limited (Li et al., 2017).

Based on the previous research findings, this paper focused on using basalt textile to reinforce fine-grained concrete, while short AR-glass fibers were added to the BTRC matrix to achieve improved load-bearing capacity and optimized cracking patterns. Studies on the basic mechanical properties of short fiber reinforced cement-based materials were carried out to determine the best fiber content. The four-point bending test of BTRC specimens was performed with the aim of evaluating the effect of textile layer and fiber length on the flexural behavior.

MECHANICAL PROPERTIES OF EXPERIMENTS OF CEMENT-BASED MATRIX WITH SHORT FIBERS

Material Characteristics

To research the impact of short fibers on mechanical properties of cement-based materials, AR-glass fibers of three different lengths (i.e., 6, 12, and 18 mm) are selected as reinforcing materials. The relative density of AR-glass fibers used in the experiment is 2.7 g/m^3, the tensile strength is 2,500∼3,500 MPa, the elastic modulus is 80.4 N/mm^2, and the fiber diameter is 15 μm. The physical and mechanical properties of AR-glass fibers are provided by the manufacturer. Each fiber bundle is composed of a large number of fiber monofilaments under the microscope. The primary mix proportion of the cement-based matrix adopted in this experiment is cement: sand: water: water reducer = 1: 1.36: 0.34: 0.016. In the test, ordinary Portland cement of 42.5

TABLE 1 | Fiber content of each type of fine-grained concrete.

Number	φ /wt%	φ /wt%	φ /wt%
PC	—	—	—
GF6-2	2	—	—
GF6-5	5	—	—
GF6-8	8	—	—
GF12-2	—	2	—
GF12-5	—	5	—
GF12-8	—	8	—
GF18-2	—	—	2
GF18-5	—	—	5
GF18-8	—	—	8

R is used, medium-size ordinary river sand is used according to the code "Standard for Quality Control of Concrete (GB50164-2011, 2011)," and water reducer of JM-PCA (I) with 18–22% water-reducing rate is chosen.

Specimen Design and Testing

To consider the effects of both the content and the length of AR-glass fibers on the mechanical properties of cement-based materials (i.e., fine-grained concrete) in this study. Test cases of 10 groups are considered and designed, and the design parameters of specimens are presented in **Table 1**. In the table, PC denotes plain concrete; GF denotes glass fiber reinforced concrete, the subsequent numbers represent the length of short fibers, and the number at the end represents the mass content of short fibers. Three mass contents with 2, 5, and 8% of short fibers are chosen for this experiment, and the corresponding volume content obtained through the conversion of fiber mass and density are 0.6, 1.5, and 2.5%, respectively. It is important to note that the fine-grained concrete is difficult to deform and cast when the fiber mass content is up to 8%. Hence, the maximum mass content of AR-glass fiber in the fine-grained concrete is determined as 8% in this study.

The compressive, bending and splitting tensile tests of fine-grained concrete for each design case in **Table 1** were carried out, aiming to determine the effects of short fibers on the compressive strength, bending strength and splitting tensile strength of concrete. According to Chinese codes "Standard for Test Method of Performance on Building Mortar" (JGJ/T70-2009, 2009) and "Method of Testing cements-Determination of Strength" (GBT17671-1999, 1999), the compression and splitting specimen is a cube with 70.7 mm × 70.7 mm × 70.7 mm, and the bending specimen is a prism with dimensions of 40 mm × 40 mm × 160 mm. Three specimens were prepared for each design case for testing to ensure the validity of the test results. After the specimen was formed for 24 h, the mold was removed, and specimens were put into water for curing at room temperature for 28 days. Note that the feeding sequence and mixing process should be strictly controlled in order to prevent the "agglomeration" phenomenon of uneven dispersion of fibers in concrete. Firstly, the sand and cement were added to the mixing bucket and fully stirred. Then, the short fibers were gradually added to the mixture while stirring. Finally, the water and water reducer were added into the mixture.

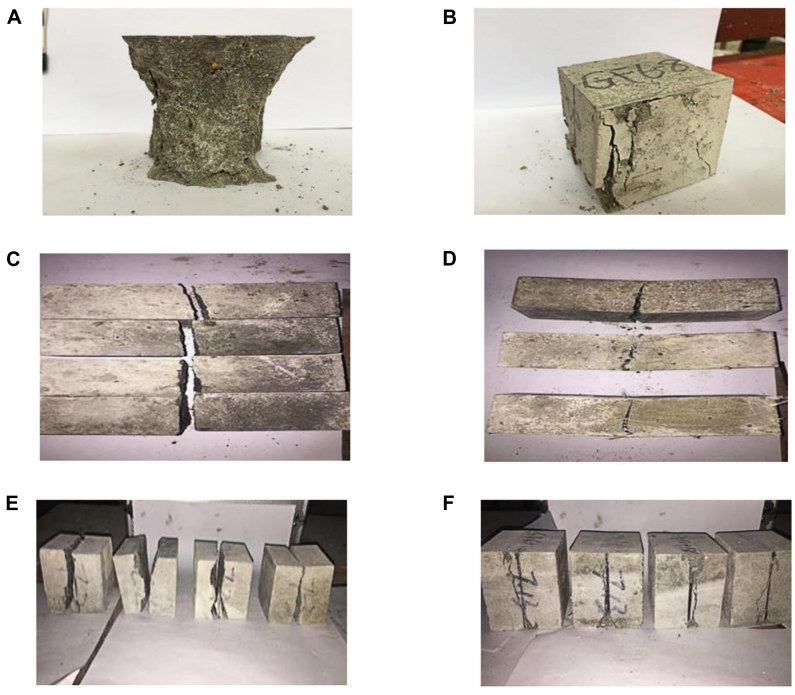

FIGURE 1 | Typical failure modes of fine-grained concrete specimens. **(A)** Compression failure without fibers, **(B)** compression failure with fibers, **(C)** bending failure without fibers, **(D)** bending failure with fibers, **(E)** splitting tensile failure without fibers, and **(F)** splitting tensile failure with fibers.

TABLE 2 | Strength of fine-grained concrete reinforced with AR-glass fibers (28 days).

Specimen	f_{cu} (MPa)	f_{fu} (MPa)	f_{tu} (MPa)
PC	38.5	9.3	3
GF6-2	37.5	9.8	3.7
GF6-5	38.6	11.9	4.6
GF6-8	38.8	14	4.1
GF12-2	38	11.4	3.8
GF12-5	39	14	3.9
GF12-8	40.3	14.4	4.6
GF18-2	39.7	12.3	5.2
GF18-5	41.5	13.3	5.4
GF18-8	41	15	4.7

Experimental Results and Analysis

Failure Modes

Figure 1 presents the failure patterns of specimens both with and without short fibers. The compression failure mode is exhibited in **Figures 1A,B**. The final failure pattern of specimens without fiber was characterized by an inverted cone due to the large area of concrete spalling in the middle part of the specimens, exhibiting an obvious brittle characteristic. While for AR-glass fiber reinforced concrete, the integrity of the specimen was maintained well, a trend of outward expansion of the core concrete could still be observed. The fracture surface of the AR-glass fiber reinforced specimen was connected through fiber and partially un-cracked concrete when bending and splitting failure occurred. By contrast, PC specimens were divided into two parts and entirely without connection between the failure sections, as shown in **Figures 1C,D** for bending failure, as well as **Figures 1E,F** for splitting tensile failure. It is worth noting that similar conclusions have been obtained in previous studies on fiber reinforced concrete (Li et al., 2010; Jiang et al., 2014).

Mechanical Properties

Table 2 presents the measured average values of the compressive strength (f_{cu}), bending strength (f_{fu}) and splitting strength (f_{tu}) of AR-glass fiber reinforced fine-grained concrete. As the table shows, AR-glass fibers could significantly improve the mechanical properties of fine-grained concrete. Generally, the compressive strength and bending strength, as well as splitting strength of AR-glass fiber reinforced concrete specimens were markedly improved when adding 5% or more short fibers. Moreover, the improvement presented an obvious increase with the increase of fiber length. The maximum improvement of compressive strength, bending strength and splitting strength for the fiber reinforced concrete specimens with 18-mm AR-glass fibers were 7.79, 61.29, and 80.0% compared with unreinforced concrete specimens respectively, which were generally higher than those with 6 and 12 mm AR-glass fibers.

The mechanical properties of AR-glass fiber reinforced concrete were further analyzed. The relationships on compressive strength, bending strength and splitting strength of fiber reinforced concrete specimens versus fiber contents, respectively, are presented in **Figure 2**. The compressive and splitting strength of AR-glass fiber reinforced concrete increased initially, and then decreased with the increase of fiber content, while the bending strength increased with the increase of fiber content. It is worth noting that the fluidity of concrete during pouring is relatively poor when the fiber content is more than 5%. Hence, the best improvement of the comprehensive mechanical properties of cement-based materials was obtained when the AR-glass fiber mass content was about 5%. In addition, the fiber length (i.e., length-diameter ratio) was also an important factor affecting the mechanical properties of cement-based materials. The reinforcement effect of 18 mm AR-glass fiber was better than that of 12 and 6 mm fibers, especially in the improvement of compressive and splitting strength of concrete specimens.

FLEXURAL PROPERTIES OF BTRC SHEETS WITH SHORT FIBERS

Experimental Program

Specimens Design and Material Properties

To study the influences of both short AR-glass fiber length and the number of textile layers on the flexural behavior of basalt fiber textile reinforced concrete (BTRC) sheets, a total of 20

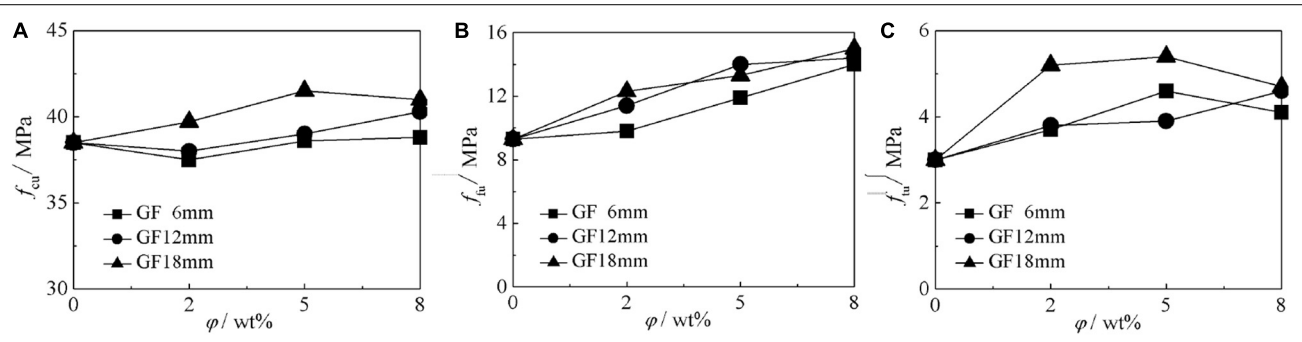

FIGURE 2 | Strength of fine-grained reinforced concrete varies with the contents of AR-glass fiber. **(A)** Compression strength, **(B)** bending strength, and **(C)** splitting tensile strength.

TABLE 3 | Basalt textile reinforced concrete sheets.

Specimen	Matrix	10 mm × 10 mm textile layer
PC-0	PC	0
PC-1	PC	1
PC-2	PC	2
PC-3	PC	3
PC-4	PC	4
GF6-5-0	GF6-5	0
GF6-5-1	GF6-5	1
GF6-5-2	GF6-5	2
GF6-5-3	GF6-5	3
GF6-5-4	GF6-5	4
GF12-5-0	GF12-5	0
GF12-5-1	GF12-5	1
GF12-5-2	GF12-5	2
GF12-5-3	GF12-5	3
GF12-5-4	GF12-5	4
GF18-5-0	GF18-5	0
GF18-5-1	GF18-5	1
GF18-5-2	GF18-5	2
GF18-5-3	GF18-5	3
GF18-5-4	GF18-5	4

group specimens were prepared for the four-point bending test by adjusting the length of short fibers in the BTRC matrix and the number of design textile layers. Note that a 5% short fiber content was adopted uniformly to reinforce the BTRC matrices for the best reinforcement effects according to the study mentioned in section "Mechanical properties of experiments of cement-based matrix with short fibers." The experimental program of the BTRC sheets is shown in **Table 3**, where "PC-x" represents a plain concrete sheet without short fibers, and the subsequent number is the number of textile layers. For "GFx-x-x," GF and the following number represents the BTRC sheets with short fibers and its length, the middle number is the fiber content, and the final number is textile layers.

The raw material and mixing proportion of the BTRC matrix has been introduced in section "Material characteristics." The basalt textile fabric used as the composite internal reinforcement in this research is a warp knitted structure with a mesh size of 10 mm, roving composed of 400 fiber filaments and an average measured tensile strength of 2393.6 MPa. The properties of basalt textile materials are summarized in **Table 4**.

Specimen Preparation and Testing

Rectangular solid BTRC sheets (i.e., 400 mm long, 100 mm wide, and 20 mm thick) were produced for four-point bending tests using a lamination technique. The laminating process started with the spreading of a thin concrete layer on the bottom of the mold, and then the first textile sheet was laid on this fresh concrete layer and then partially pressed in and smoothed. These production steps were repeated until all reinforcing layers (e.g., 2, 3, or 4 layers in this study) were placed and incorporated into the finely grained concrete, and it should be verified that the warp rovings in specimens were parallelized with the longitudinal surface of specimens. Then, the specimens were covered with

TABLE 4 | Physical and mechanical properties of basalt textile.

Type	Area of a single roving (mm^2)	Tensile strength (MPa)	Modulus of elasticity (GPa)	Elongation (%)	Density (g/cm^3)	Linear density (tex)
Basalt	0.53	2,400	91	11.6	2.63	132

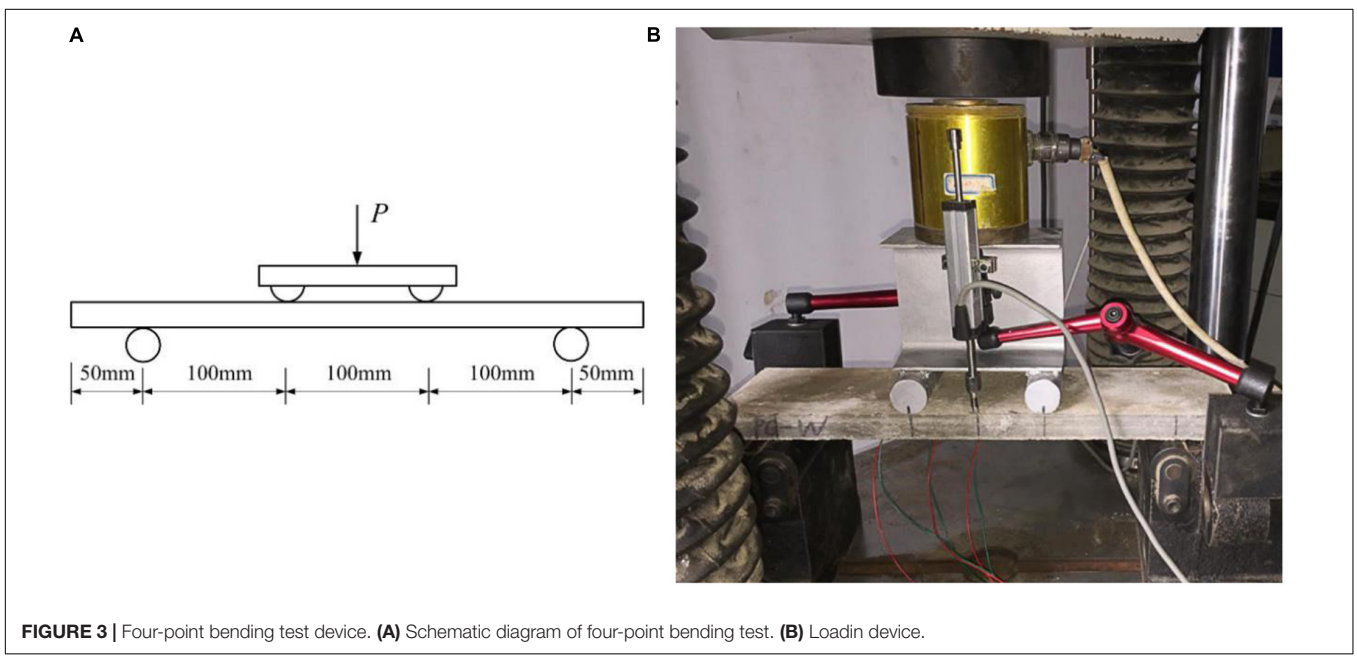

FIGURE 3 | Four-point bending test device. **(A)** Schematic diagram of four-point bending test. **(B)** Loadin device.

plastic film to prevent the evaporation of water after casting. The molds were removed after 24 h, then the specimens were placed in the standard curing condition for 28 days for testing. For each group, the same three specimens were poured for available test results.

The four-point bending tests of BTRC specimens were carried out by a 30-t microcomputer controlled electro-hydraulic universal servo testing machine. The test was performed under displacement control at a constant rate of 0.5 mm/min. The span length of the flexural loading was 100 mm. The loading schematic diagram is shown in **Figure 3**.

Experimental Results and Analysis

Failure Mode

Figure 4 presents the failure pattern of PC specimens and BTRC specimens. PC specimens (e.g., PC-0) were destroyed immediately and split into two parts without any warning once the specimens cracked during the testing, as shown in **Figure 4** (a). For the BTRC specimens without short fibers (e.g., PC-3), The final failure mode was characterized by 2–3 main cracks through the section of the specimen in the pure bending zone, and the sheets were not divided into two parts due to the connection of the continuous fiber bundles of textile, as shown in **Figure 4B**. This indicated that the brittle failure characteristic of specimens was improved to some extent as the textile meshes were adopted as reinforced materials. Multiple fine cracks steadily appeared and propagated on BTRC specimens after adding short fibers, as shown in **Figure 4C**. The specimens presented a multi-crack cracking failure pattern due to the combination function of long continuous textile filaments and random short AR-glass fibers. The results indicated that the addition of short fibers could effectively improve the brittle failure characteristic and deformability of BTRC specimens.

Moreover, to quantitatively analyze the influence of the number of textile layers and the length of short fibers on the cracking behavior of BTRC specimens, **Figures 5**, **6** illustrate that the number of cracks varies with the number of textile layers and the length of short fibers. More cracks were observed on the specimens with basalt textile used in comparison with PC specimens which exhibited only one mid-span main crack. The number of cracks increased with the increase of the number of textile layers in general, and the number of cracks increased to 5∼7 with four-layer textile, as shown in **Figure 5**. This was due to the textile being able to restrain and delay the development of cracks. In addition, the number of cracks for short AR-glass fiber reinforced BTRC sheets was more than that of sheets without short fibers, and the number also increased with the increase of fiber length, as shown in **Figure 6**. These results indicated that short AR-glass fibers played a good bridging role in fine-grained concrete, making the stress distribution inside the concrete more even and presenting a good multi-crack cracking mode.

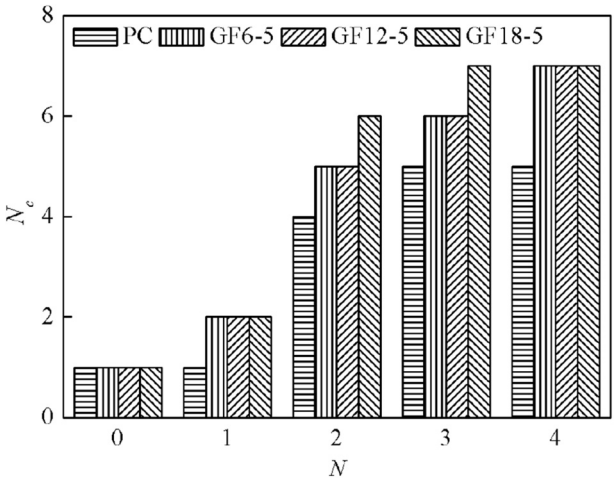

FIGURE 5 | Relationship between the number of cracks and textile layers.

Bearing Capacity and Deformation

The four-point bending test results of all specimens are summarized in **Table 5**, mainly including cracking load, ultimate

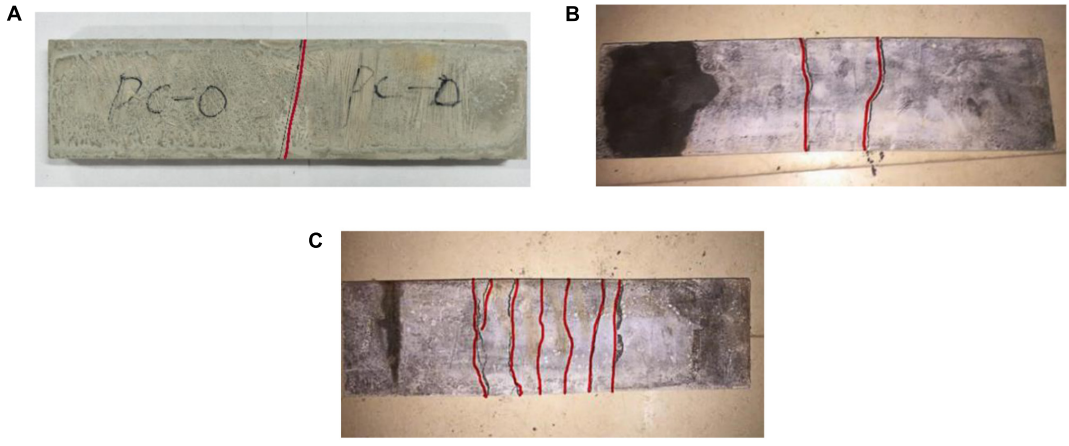

FIGURE 4 | Sheet failure modes. **(A)** PC sheet. **(B)** BTRC sheet without short fibers. **(C)** BTRC sheet with short fibers.

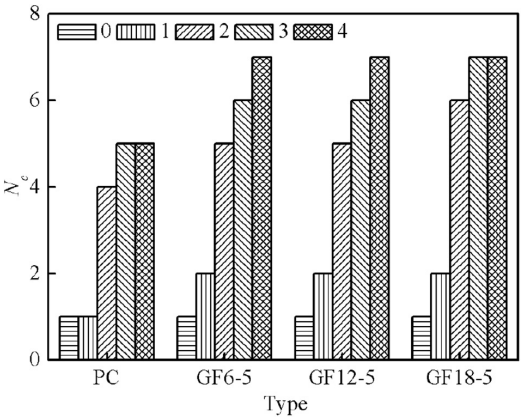

FIGURE 6 | Relationship between the number of cracks and short fiber length.

load and corresponding deformation. As a whole, the BTRC specimens experienced a significant increase in cracking load and ultimate load compared with the control specimen (i.e., PC-0). The increment also showed a positive correlation with the increase of textile layers, and the maximum increment may reach up to 22.4 and 62.1%, respectively, when four textile layers were used. Meanwhile, the ultimate deformation also improved significantly with the increase of textile layers, the maximum deformation was up to 6.15 mm for BTRC specimens when four layers of textile were adopted. The increment was more than 15 times that of the control specimen, which indicates that the ultimate bearing capacity and deformability could obtain a noticeable improvement when enough textile is adopted. Note that there was little improvement in ultimate load and deformation when the fine-grained concrete sheets are reinforced with two or fewer layers of textile.

Moreover, the cracking load and ultimate load of BTRC specimens with short fibers were further improved in comparison with those without short fibers. Particularly, the cracking load's greatest increase was by 106%. It can be seen that the cracking load of the specimens generally presented a rising trend with the increase of fiber length, which indicated that the longer fibers provided a stronger cracking resistance role in concrete. The principle behind this result is that longer short fiber provides a greater contact surface between fibers and the matrix, which strengthens the cohesive force and requires more energy to pull out the fiber, thereby delaying the development of cracks. In addition, the short AR-glass fibers could also improve the ultimate bearing capacity. This is because the dispersed fibers helped to improve the stress transfer capacity inside the matrix, and an even and gentle stress distribution in sheets were achieved to improve its ultimate bearing capacity.

Figure 7 presents the effects of the number of textile layers and short fibers on the load-bending deformation curves of BTRC sheets. Take **Figure 7D** as the example, which shows the load-deformation curves of BTRC specimens with 18 mm AR-glass fibers and textile ranging from 0 to 4 layers. With regards to BTRC specimens, the curve response is generally characterized by three different branches defined as linear, hardening, and failure. Initially, a linear stage with a similar slope to that of all specimens subjected to a relatively low load is observed. Subsequently, the curve begins to enter the non-linear stage because the fracture is initiated by matrix

TABLE 5 | The main results of sheet bending tests.

Number	Crack load (N)	Cracking displacement Δ_{cr} (mm)	Ultimate load (N)	Ultimate displacementΔ_p (mm)	Displacement ductility coefficient
PC-0	945.94	0.36	945.94	0.36	1.0
PC-1	799.59	0.37	799.59	0.37	1.0
PC-2	1048.60	0.66	1048.60	0.66	1.0
PC-3	1090.21	0.44	1450.00	5.55	12.61
PC-4	1157.39	0.35	1533.07	6.15	17.57
GF6-5-0	1129.74	0.40	1144.56	0.44	1.1
GF6-5-1	1241.40	0.35	1423.29	0.98	2.8
GF6-5-2	1013.10	0.50	1640.79	7.31	14.62
GF6-5-3	788.73	0.32	1466.79	7.69	24.03
GF6-5-4	1181.10	0.45	2162.69	6.53	14.51
GF12-5-0	1206.00	0.35	1345.37	0.61	1.74
GF12-5-1	1644.76	0.43	1644.76	0.43	1.0
GF12-5-2	1107.00	0.40	1741.67	4.79	11.98
GF12-5-3	1388.76	0.40	2021.34	7.14	17.85
GF12-5-4	1565.68	0.42	2234.87	3.79	9.02
GF18-5-0	961.69	0.42	1173.24	1.36	3.24
GF18-5-1	1185.14	0.34	1573.61	4.13	12.15
GF18-5-2	1276.10	0.40	1879.05	4.01	10.03
GF18-5-3	1344.22	0.40	2011.43	3.04	7.6
GF18-5-4	1268.17	0.40	2254.59	4.45	11.13

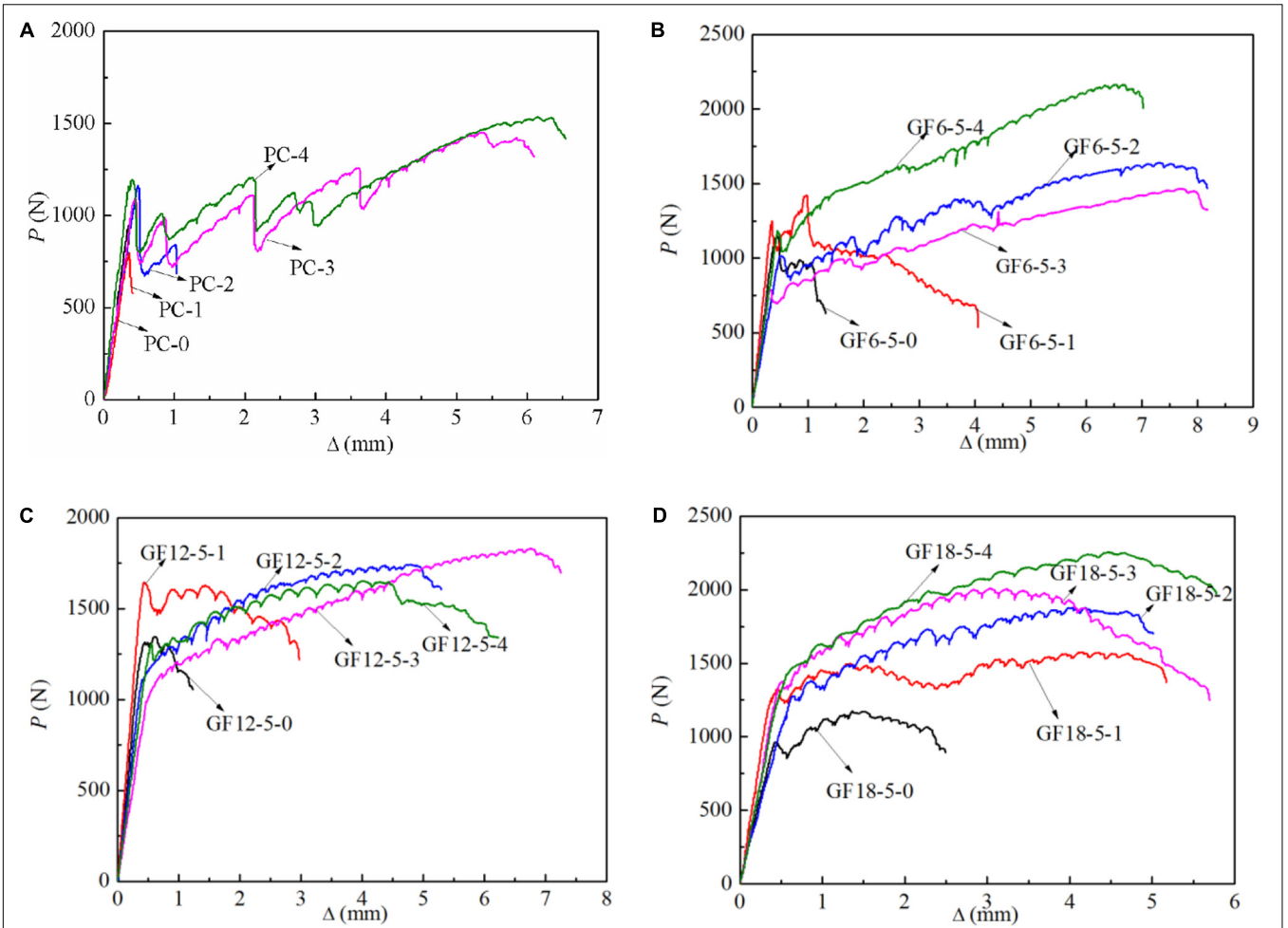

FIGURE 7 | Relationship of load-deformation curves and the number of textile layers. **(A)** PC, **(B)** GF6-5, **(C)** GF12-5, and **(D)** GF18-5.

cracking with the increment of the load, but the bearing load is also increased with deformation increasing due to the tensile bearing of textile reinforcement, which shows the characteristics of curve-hardening. Finally, the curve begins to decline and fail when the textile reinforcement reaches the ultimate tensile strength, and the specimen completely loses its bearing capacity rapidly. For comparison, the curves of concrete sheets with textile layers are higher than that without textile layers, and the greater ultimate load and deformation are obtained for the BTRC specimens with the increase of textile layers.

In addition, it can be seen by comparing **Figures 7A–D** that the higher and flatter curve response was observed following the application of short fibers, and the increasing of short fiber length had a positive effect on the enhancing of curve response on the whole. This indicated that the addition of short fibers improved the load-bearing and deformation capacity of BTRC, and the increment increased with an increase of the fiber length. This can be explained that the bridging effects of short fibers can enhance the stress transferring in the interface between the textile and cracked matrix.

Nominal Displacement Ductility and Toughness

According to the load-deformation curves of BTRC specimens shown in **Figure 7**, the cracking of the matrix can be considered as an indication of the nominal yielding of the specimen due to the occurrence of non-linear transition. Moreover, there is not a definite yield point for BTRC composites because of the linear elastic constitutive relation of basalt fiber textile materials. Therefore, the nominal displacement ductility coefficient of BTRC sheets can be calculated by the following formula:

$$\mu_{\Delta} = \frac{\Delta_p}{\Delta_{cr}} \tag{1}$$

Where μ_{Δ} is the displacement ductility coefficient of BTRC specimens, Δ_p is ultimate displacement, and Δ_{cr} is the nominal yielding displacement corresponding to the displacement of matrix cracking. The specific method to determine the displacement ductility coefficient is shown in **Figure 8**, and the specimen GF 12-5-3 is taken as an example. The calculation results of displacement ductility coefficients for all BTRC sheets are listed in **Table 5**.

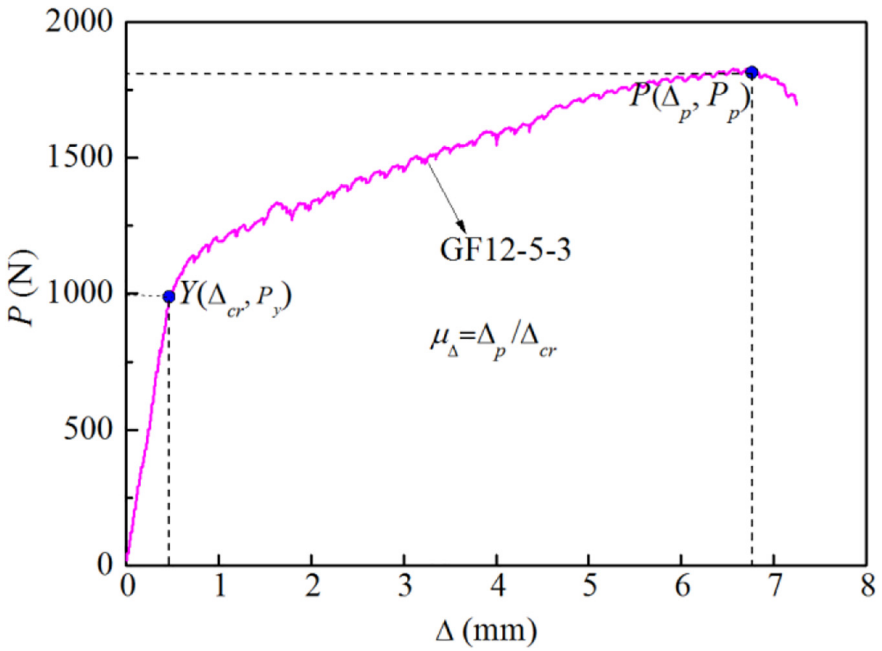

FIGURE 8 | Determination of displacement ductility coefficient for BTRC sheet.

From **Table 5**, it can be observed that the displacement ductility coefficients of BTRC specimens is obviously increased with the increase of the number of textile layers, and is also improved significantly with the addition of short fibers in the matrix. The maximum ductility coefficient is as high as 24.03 when the BTRC sheet is reinforced with an appropriate amount of textile and short fibers. By contrast, the effect trend of short fiber length on the displacement ductility coefficient is not very clear, but generally presents an initial rising trend with the increase of the short fiber length. It can be explained that the homogeneity of bridging role is affected not only by the length but also by the random and uncertainty distribution characteristics of short fibers in the matrix of BTRC.

To intuitively analyze the contributions of continuous textile and short fibers to the flexural properties of the fine-grained concrete sheets, the toughness indexes I_5, I_{10}, I_{20} and I_{30} recommended by ASTM C1018 (1997) are adopted to evaluate the flexural toughness of BTRC sheets at different response stages. The calculation method of flexural toughness of BTRC sheet is shown in **Figure 9**, and the specimen GF12-5-3 is taken as an example. The computational formula is as follows:

$$I_m = \frac{\Omega_{n\delta_{cr}}}{\Omega_{\delta_{cr}}} \tag{2}$$

Where I_m is the flexural toughness index, the subscript m is 5, 10, 20, and 30 respectively; $\Omega_{n\delta_{cr}}$ is the area enclosed by X-axis and the curve OP_2, OP_3, OP_4 and OP_5 in **Figure 9** respectively, and the subscript $n\delta_{cr}$ is represented as the displacement of point P_2, P_3, P_4, and P_5 and equal to 3.0, 5.5, 10.5, and 15.5 times of initial cracking displacement$\delta_{cr}$of the specimen, respectively, $\Omega_{\delta_{cr}}$ is the area enclosed by X-axis and the curve OP_1, and the subscriptδ_{cr} is represented as the displacement of point P_1 and equal to the initial cracking displacementδ_{cr} .

According to the Eq. 2, flexural toughness indexes of all BTRC sheets for different response stages were calculated and compared in **Figure 10**, the influences of the number of textile layers and short AR-glass fiber length were also considered. As shown in **Figure 10**, the toughness indexes of I_5, I_{10}, I_{20}, and I_{30} of the BTRC sheets with short AR-glass fibers are obviously higher than that without short fibers (i.e., PC specimens), and the improvement tendency increases with the increasing of short fiber length on the whole. These suggest that the bridging role

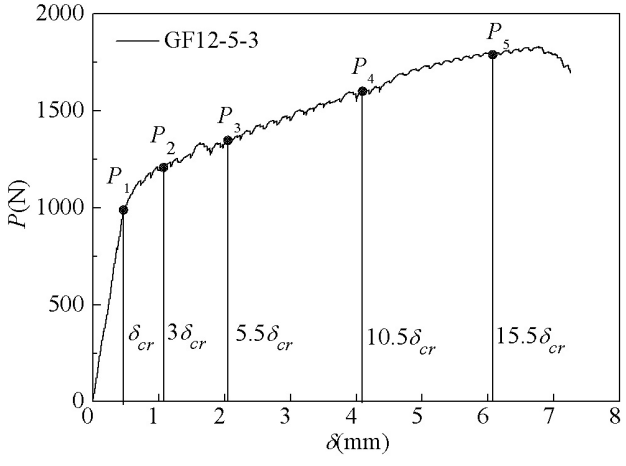

FIGURE 9 | Calculations of flexural toughness indexes of BTRC.

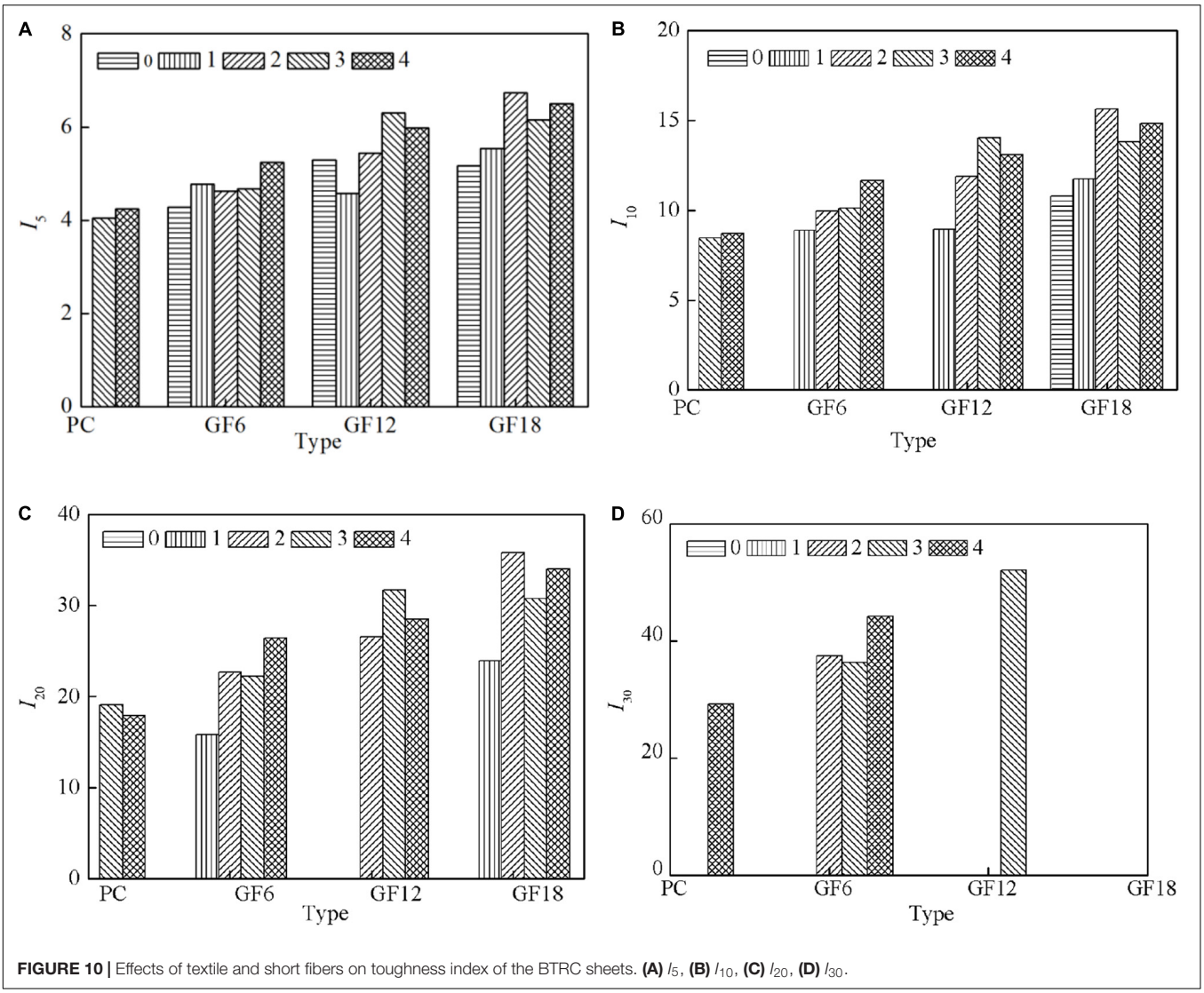

FIGURE 10 | Effects of textile and short fibers on toughness index of the BTRC sheets. **(A)** I_5, **(B)** I_{10}, **(C)** I_{20}, **(D)** I_{30}.

and stress transferring effect of short fibers have a positive contribution to the flexural toughness of BTRC sheets at each deformation stage, and the contribution is greater for the longer fibers due to the greater ability of crossing cracks. Moreover, it also can be seen from the figure that the flexural toughness indexes of the BTRC sheets increase with the increasing of the number of textile layers when the specimens are reinforced with enough textile and suitable short fibers. Note that the toughness indexes of I_5, I_{10}, I_{20}, and I_{30} of some BTRC specimens (e.g., PC-0, PC-1, PC-2, and so on) are not shown in the figure, which can be explained by the fact that these BTRC specimens were destroyed with smaller deformation and demonstrated a poor toughness because the specimens were reinforced without enough textile and short fibers. Therefore, the influence rules of textile and short fibers on flexural toughness indexes of I_5, I_{10}, and I_{20} are relatively well defined, but those of I_{30} seem uncertain due to the larger deformations of specimens. This is because most short AR-glass fibers are broken or pulled out in the matrices when the deformation of the specimens increases to a certain extent. Meanwhile, the majority of textile between the cracks is inclined to rupture due to the stress concentration effect.

REINFORCEMENT MECHANISM OF MULTI-SCALE FIBERS

The BTRC sheets with high-toughness mainly rely on the compound reinforcement effects of continuous basalt fiber textiles and short AR-glass fibers, and the reinforcement mechanism of two types of fibers on fine-grained concrete should be illustrated from macro and micro perspectives, respectively. Micromorphology and distribution of short AR-glass fibers on the fracture surfaces of BTRC sheets are investigated by means of Scanning Electron Microscope (SEM), as shown in **Figures 11A–C**. From the **Figures 11A,B**, it can be seen that the short fibers in cement-based materials mainly play the roles of crack resistance and bridging, the stress between cracks and internal pores of the matrix can be transferred for delaying

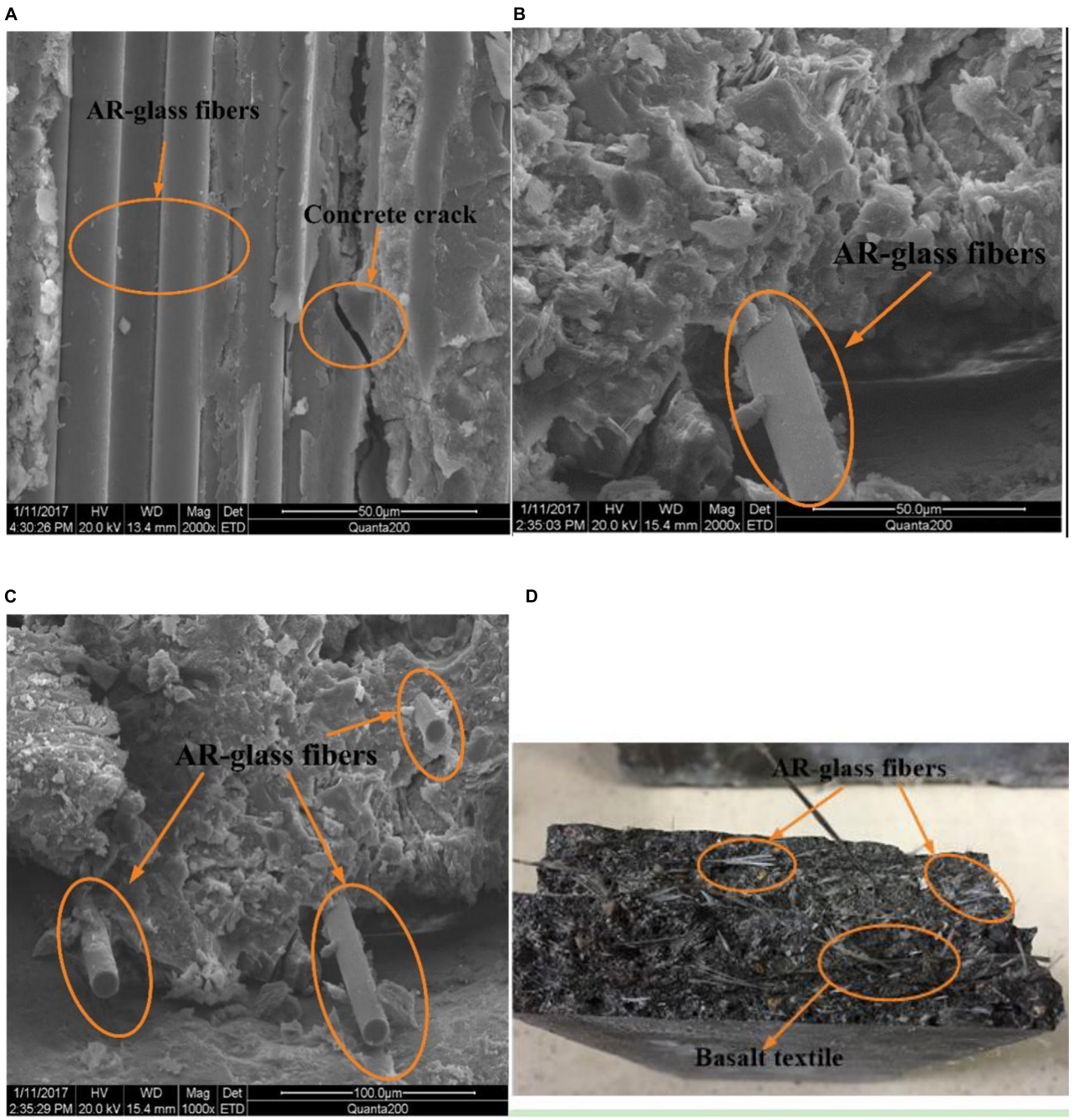

FIGURE 11 | Morphology observations of short fibers and textile in fine-grained concrete. **(A)** Cracking resistance of short fiber, **(B)** bridging role of short fiber, **(C)** uniformly distributed of short fibers, and **(D)** recombination of short fibers and textile.

the destroy. Also, the uniform dispersion of short fibers (as shown in **Figure 11C**) in the matrix is also beneficial to its reinforcement effect. For the continuous fiber textiles, the reinforcement effect mainly reflected in improving the macro-flexural performance of fine-grained concrete sheets by means of the mechanical characteristic of bearing-directed, and the textile may be viewed as the reinforcing material in the concrete. In general, for BTRC sheets without short fibers, the continuous fiber bundle of textile is inclined to fracture due to stress concentration effect once the concrete matrix cracked. While for the BTRC sheets with short fibers, the tensile property of the continuous fiber bundle can play a part because the effect of stress concentration between cracks is released due to the energy dissipation of random distributed short fibers by sliding, friction and self-fracture during the process of loading. Furthermore, the bonding force between the textile

and cement-based matrix could be enhanced through the "cross-linking" between textile and short fibers, and the relative slip between the fiber bundle and the matrix is further prevented, thereby improving the mechanical properties of the BTRC sheets. **Figure 11D** show the recombination effect of short AR-glass fibers and continuous basalt textile on the fracture surface of the BTRC sheet at the macro level. This suggests that the structural properties such as micro-cracking and macro-stress in cement-based materials can be improved by adopting an appropriate amount of textile and short fibers for compound reinforcing.

CONCLUSION

The experimental investigations focusing on the mechanical properties of short fiber reinforced fine-grained concrete and BTRC sheets both with and without short fibers were performed. From the findings, the following conclusions could be drawn:

(1) The load bearing capacity and deformability of fine-grained concrete are improved markedly by the reinforcing effect of short AR-glass fibers. The mechanical properties increase significantly with the increase of the content and length of short fibers, and the maximum improvement of bending strength and splitting strength are up to 61.3 and 80%, respectively. The best improvement of the comprehensive mechanical properties of the concrete matrix is obtained when the AR-glass fiber mass content is about 5%.

(2) The flexural strength and deformation capacity of BTRC sheets are greatly improved with the compound reinforcement of basalt textile and short AR-glass fibers, and the improved efficiency increases with the increasing of the number of textile layers and short fiber length. The maximum increment of load bearing capacity (i.e., ultimate load) and nominal displacement ductility of BTRC sheets may reach up to 1.4 times and 23 times of the sheets without reinforcing by the basalt textile and short AR-glass fibers, respectively. The cracking loads of BTRC sheets are improved remarkably with the addition of short fibers, and the maximum increment may exceed 100% compared to that without short fibers.

(3) The BTRC sheets with high toughness can be obtained by adopting an appropriate amount of continuous textile and short fibers for compound reinforcing. The continuous textile plays a reinforcing role in the concrete matrix by means of the mechanical characteristic of bearing-directed, and the short fibers distributed randomly in the matrix mainly to restrain micro and macro-cracks and weaken stress concentration effect triggered by cracking.

DATA AVAILABILITY STATEMENT

The raw data supporting the conclusions of this article will be made available by the authors, without undue reservation, to any qualified researcher.

AUTHOR CONTRIBUTIONS

All authors listed have made a substantial, direct and intellectual contribution to the work, and approved it for publication.

FUNDING

The work in this paper was financed by the Natural Science Foundations of China (Nos. 51508154, 51978125, 51678104, and 51909238), the Fundamental Research Funds for the Central Universities (2019B13614), China Postdoctoral Science Foundation (2020M670787), the National Key Research and Development Plan (2017YFC0404902), and the Priority Academic Program Development of Jiangsu Higher Education Institutions. The authors wish to express their gratitude for these financial supports.

REFERENCES

Al-Salloum, Y., Siddiqui, N., Elsanadedy, H., Abadel, A., and Aqel, M. (2011). Textile-reinforced mortar versus FRP as strengthening material for seismically deficient RC beam-column joints. *J. Compos. Constr.* 15, 920–933. doi: 10.1061/(ASCE)CC.1943-5614.0000222

ASTM C1018 (1997). *Test Method for Flexural Toughness and First-Crack Strength of Fiber Reinforced Concrete (Using Beam with Third-Point Loading)*. West Conshohocken: ASTM Internation, 544–551.

Barhum, R., and Mechtcherine, V. (2012). Effect of short, dispersed glass and carbon fibres on the behavior of textile-reinforced concrete under tensile loading. *Eng. Fract. Mech.* 92, 56–71. doi: 10.1016/j.engfracmech.2012.06.001

Barhum, R., and Mechtcherine, V. (2013a). Influence of short dispersed and short integral glass fibres on the mechanical behaviour of textile-reinforced concrete. *Mater. Struct.* 46, 557–572. doi: 10.1617/s11527-012-9913-3

Barhum, R., and Mechtcherine, V. (2013b). "Multi-level investigations on behavior of textile reinforced concrete with short fibers under tensile loading," in *8th International Conference on Fracture Mechanics of Concrete and Concrete Structures (FraMCoS-8)*, Toledo.

Carmisciano, S., Rosa, I., Sarasini, F., Tamburrano, A., and Valente, M. (2011). Basalt woven fiber reinforced vinylester composites: flexural and electrical properties. *Mater. Des.* 32, 337–342. doi: 10.1016/j.matdes.2010.06.042

Deng, M. K., Dong, Z. F., and Zhang, C. (2020). Experimental investigation on tensile behavior of carbon textile reinforced mortar (TRM) added with short polyvinyl alcohol (PVA) fibers. *Constr. Build. Mater.* 235:17801. doi: 10.1016/j.conbuildmat.2019.117801

Dhand, V., Mittal, G., Rhee, K. Y., Park, S. J., and Hui, D. (2015). A short review on basalt fiber reinforced polymer composites. *Compos. Part B* 73, 166–180. doi: 10.1016/j.compositesb.2014.12.011

Di Ludovico, M., Prota, A., and Manfredi, G. (2012). Structural upgrade using basalt fibers for concrete confinement. *J. Compos. Constr.* 14, 541–552. doi: 10.1061/(ASCE)CC.1943-5614.0000114

Du, Y., Zhang, M., Zhou, F., and Zhu, D. J. (2017). Experimental study on basalt textile reinforced concrete under uniaxial tensile loading. *Constr. Build. Mater.* 138, 88–100. doi: 10.1016/j.conbuildmat.2017.01.083

Dvorkin, D., Poursaee, A., Peled, A., and Weiss, W. (2013). Influence of bundle coating on the tensile behavior, bonding, cracking and fluid transport of fabric cement-based composites. *Cem. Concr. Compos.* 42, 9–19. doi: 10.1016/j.cemconcomp.2013.05.005

GB50164-2011 (2011). *Standard for Quality Control of Concrete*. Beijing: China Architecture and Building Press.

GBT17671-1999 (1999). *Method of Testing Cements-Determination of Strength*. Beijing: Standards Press of China.

Halvaei, M., Jamshidi, M., Latifi, M., and Ejtemaei, M. (2020). Effects of volume fraction and length of carbon short fibers on flexural properties of carbon textile reinforced engineered cementitious composites (ECCs); an experimental and computational study. *Constr. Build. Mater.* 245:118394. doi: 10.1016/j.conbuildmat.2020.118394

Hegger, J., Will, N., Bruckermann, O., and Voss, S. (2006). Load–bearing behaviour and simulation of textile reinforced concrete. *Mater. Struct.* 39, 765–776. doi: 10.1617/s11527-005-9039-y

Hinzen, M., and Brameshuber, W. (2009). "Improvement of serviceability and strength of textile reinforced concrete by using short fibers," in *4th Colloquium on Textile Reinforced Structures (CTRS4)*, Dresden, 261–272.

Isabella, G. C., Anna, M., Giulio, Z., Matteo, C., and Marco, P. (2013). Erratum to: textile reinforced concrete: experimental investigation on design parameters. *Mater. Struct.* 46, 1953–1971. doi: 10.1617/s11527-013-0017-5

JGJ/T70-2009 (2009). *Standard for Test Method of Performance on Building Mortar*. Beijing: China Architecture and Building Press.

Jiang, C. H., Fan, K., Wu, F., and Chen, D. (2014). Experimental study on the mechanical properties and microstructure of chopped basalt fibre reinforced concrete. *Mater. Des.* 58, 187–193. doi: 10.1016/j.matdes.2014.01.056

Larrinaga, P., Chastre, C., Biscaia, H., and San-Jose, J. (2014). Experimental and numerical modeling of basalt textile reinforced mortar behavior under uniaxial tensile stress. *Mater. Des.* 55, 66–74. doi: 10.1016/j.matdes.2013.09.050

Li, G. Z., Ning, C., Yuan, H. Y., and Chen, J. (2010). Effect of modified polypropylene fiber on mechanical properties of cement mortar. *J. Build. Mater.* 13, 135–138.

Li, H., Liu, S., Li, G. S., Yao, Y. M., Shi, C. J., Ou, Y. F., et al. (2020). Flexural performance of basalt textile-reinforced concrete with pretension and short Fibers. *J. Mater. Civ. Eng.* 32:04020004. doi: 10.1061/(asce)mt.1943-5533.0003077

Li, Q., and Xu, S. (2011). Experimental research on mechanical performance of hybrid fiber reinforced cementitious composites with polyvinyl alcohol short fiber and carbon textile. *J. Compos. Mater.* 45, 5–28. doi: 10.1177/0021998310371529

Li, T., Zhang, Y., and Dai, J. G. (2017). Flexural behavior and microstructure of hybrid basalt textile and steel fiber reinforced alkali-activated slag panels exposed to elevated temperatures. *Constr. Build. Mater.*s. 152, 651–660. doi: 10.1016/j.conbuildmat.2017.07.059

Liu, Q., Shaw, M. T., Parnas, R. S., and McDonnell, A. M. (2006). Investigation of basalt fiber composite mechanical properties for applications in transportation. *Polym. Compos.* 27, 41–48. doi: 10.1002/pc.20162

Pellegrino, C., and D'Antino, T. (2013). Experimental behaviour of existing precast prestressed reinforced concrete elements strengthened with cementitious composites. *Compos. Part B* 55, 31–40. doi: 10.1016/j.compositesb.2013.05.053

Rambo, D., Silva, F., Filho, R., and Gomes, O. (2015). Effect of elevated temperatures on the mechanical behavior of basalt textile reinforced refractory concrete. *Mater. Des.* 65, 24–33. doi: 10.1016/j.matdes.2014.08.060

Shen, L. H., Wang, J. Y., and Xu, S. L. (2016). Experimental study on bending mechanical behavior of textile reinforced concrete thin-plates with short dispersed fibers. *J. Build. Struct.* 37, 98–107. doi: 10.14006/j.jzjgxb.2016.10.012

Szabó, J. S., and Czigány, T. (2003). Static fracture and failure behavior of aligned discontinuous mineral fiber reinforced polypropylene composites. *Polym. Test* 22, 711–719. doi: 10.1016/S0142-9418(03)00005-9

Wang, Y. L., Chen, G. P., Wan, B. L., Cai, G. C., and Zhang, Y. W. (2020). Behavior of circular ice-filled self-luminous FRP tubular stub columns under axial compression. *Constr. Build. Mater.* 232:117287. doi: 10.1016/j.conbuildmat.2019.117287

Yin, S. P., Wang, B., Qiang, D. F., and Wang, X. X. (2016). Mechanical performance of textile reinforced concrete under chloride salt dry-wet cycle. *J. Build. Mater.* 19, 752–757.

Yin, S. P., Xu, S. L., and Lv, H. L. (2014). Flexural behavior of reinforced concrete beams with TRC tension zone cover. *J. Mater. Civ. Eng* 26, 320–330. doi: 10.1061/(asce)mt.1943-5533.0000811

Yin, S. P., Yu, Y., and Na, M. W. (2019). Flexural properties of load-holding reinforced concrete beams strengthened with textile-reinforced concrete under a chloride dry–wet cycle. *J. Eng. Fibers Fabr.* 14, 1–9. doi: 10.1177/1558925019845902

Zhu, D., Gencoglu, M., and Mobasher, B. (2009). Low velocity flexural impact behavior of AR glass fabric reinforced cement composites. *Cem. Concr. Compos.* 31, 379–387. doi: 10.1016/j.cemconcomp.2009.04.011

Zhu, D., Liu, S., Yao, Y., Li, G. S., Du, Y. X., and Shi, C. J. (2019). Effects of short fiber and pre-tension on the tensile behavior of basalt textile reinforced concrete. *Cem. Concr. Compos.* 96, 33–45. doi: 10.1016/j.cemconcomp.2018.11.015

Zhu, D., Peled, A., and Mobasher, B. (2011). Dynamic tensile testing of fabric-cement composites. *Constr. Build. Mater* 25, 385–395. doi: 10.1016/j.conbuildmat.2010.06.014

Conflict of Interest: GZ and GX were employed by the company Liaoning Provincial Traffic Planning and Design Institute Co., Ltd.

The remaining authors declare that the research was conducted in the absence of any commercial or financial relationships that could be construed as a potential conflict of interest.